Technology development roadmap for Habitable-zone exoplanet observatory (HabEx) baseline 4-m primary mirror

H. Philip Stahl[a] and Rhonda Morgan[b]

[a] NASA MARSHALL SPACE FLIGTH CENTER, HUNTSVILLE, AL 35812
[b] JET PROPULSION LABORATORY, CALIFORNIA INSTITUTE OF TECHNOLOGY, PASADINA, CA 91109

ABSTRACT

The Habitable Exoplanet Observatory (HabEx) is one of four mission concepts under study for the 2020 Astrophysics Decadal Survey. Its goal is to directly image and spectroscopically characterize planetary systems in the habitable zone around nearby sun-like stars. Additionally, HabEx will perform a broad range of general astrophysics science enabled by 115 to 2500 nm spectral range and 3 x 3 arc-minute FOV. Critical to achieving the HabEx science goals is a large, ultra-stable UV/Optical/Near-IR (UVOIR) telescope. The baseline HabEx telescope is 4-meter off-axis unobscured, diffraction limited at 400 nm with wavefront stability on the order of a few 10s of picometers. The technology readiness level (TRL) to manufacture and test the HabEx baseline primary mirror is assessed to be at TRL-6 for all but two TRL-4 technologies: 1) non-destructive process to quantify CTE homogeneity of a 4-m mirror substrate with a spatial sampling of at least 100 x 100 to better than +/- 1 ppb/K; and, 2) process to quantify self-weight gravity deflection to better than 4-nm rms over a 100 x 100 spatial sampling. This paper reviews the technology needs to manufacture the HabEx primary mirror, assesses their TRL and proposes a roadmap to mature the two remaining technologies to TRL-6.

Keywords: optical manufacture, optical test, space telescopes, astrophysics, astronomy, HabEx, exoplanets, direct imaging

1. INTRODUCTION

"Are we alone in the Universe?" maybe the most compelling science question of our generation. Per the 2010 *New Worlds, New Horizons* Decadal Report[1]: "One of the fastest growing and most exciting fields in astrophysics is the study of planets beyond our solar system. The ultimate goal is to image rocky planets that lie in the habitable zone of nearby stars." As a result, NASA is studying in detail the Habitable Exoplanet Observatory Concept (HabEx) for the 2020 Decadal Survey. HabEx has three goals: to seek out nearby worlds and explore their habitability; to map out nearby planetary systems and understand the diversity of the worlds they contain; and, to carry out observations that open up new windows on the universe from the UV through near-IR. The HabEx Science and Technology Definition Team has selected a baseline architecture of a 4-meter telescope with four science instruments (coronagraph, star-shade instrument, UV-NIR imaging multi-object slit spectrograph, and high resolution UV spectrograph) and a 52-m external star-shade occulter.

To accomplish this goal, the Survey recommended, as its highest priority medium-scale activity, a "New Worlds Technology Development Program" to "lay the technical and scientific foundations for a future space imaging and spectroscopy mission." Additionally, the National Research Council report, *NASA Space Technology Roadmaps & Prioroties*[2], states that NASA's second highest technical challenge, for expanding our understanding of the universe in which we live, is to "Develop a new generation of astronomical telescopes that enable discovery of habitable planets … by developing high-contrast imaging and spectroscopic technologies to provide unprecedented sensitivity, field of view, and spectroscopy of faint objects." Responding to these recommendations, NASA has invested in technology that will enable a potential HabEx. Currently, all HabEx enabling technologies are at TRL 4 or higher. And, all but two are predicted to be at TRL 5 by the end of 2023—a full year before the nominal start of Phase A for a HabEx mission. One technology that will not be at TRL 5 until 2024 is primary mirror fabrication. Since it is not enabling for any other proposed mission, the cost of a 4-meter monolithic primary mirror prototype is precluded from work ahead of the Decadal Survey recommendation. Thus, the time required to cast, grind and polish the mirror must wait until HabEx is recommended by the Decadal. Earlier funding could advance this technology date by a year.

This paper provides an assessment of the technology readiness level of the technology to manufacture and test the HabEx baseline primary mirror and outlines a roadmap to mature that technology to TRL-6. Section 2 defines the telescope system requirements needed to enable HabEx's mission science. Section 3 describes the telescope concept and primary-mirror assembly design details. Section 4 assesses TRL (technology readiness level) of key technologies needed to manufacture the HabEx baseline primary mirror. And, Section 5 outlines a roadmap to mature these to TRL-6.

2. OPTICAL TELESCOPE ASSEMBLY SPECIFICATIONS

The HabEx optical telescope design team used science driven systems engineering to derive the telescope assembly's engineering specifications from mission science requirements (Table 1).

Table 1: HabEx Optical Telescope Specification	
Specification	Value
Architecture	Off-Axis Unobscured Circular Aperture
Optical Design	Three-Mirror Anastigmatic
Science Instruments	On the side, in the Secondary Mirror Tower structure
Aperture Diameter	> 4.0 meters
Primary Mirror F/#	F/2.5 or slower
Diffraction Limited Wavelength	400 nm
Line of Sight Stability (Jitter)	< 0.5 milli-arc-seconds per axis
Wavefront Error Stability	1 to 250 pm depending on coronagraph and spatial frequency

Exoplanet science drives the choice of an off-axis architecture, aperture diameter and primary mirror F/#. General astrophysics' desire for a 3 x 3 arc-minute field of view (FOV) drives the choice of a three mirror anastigmatic (TMA) optical design and spectral range. Both exoplanet and general astrophysics science need 400 nm diffraction limited. The specifications that have the greatest impact on the primary-mirror assembly are off-axis configuration, aperture diameter, diffraction limited wavelength, and wavefront stability. Primary mirror F/# is needed for polarization control, but it is not a technology challenge. Jitter is a technology challenge, but for the telescope structure, not the primary mirror. And, it is solved via proper design and the use of micro-thruster technology. Thus, neither are discussed further in this paper.

2.1 Off-Axis Configuration and Aperture Diameter

Imaging habitable zone exoplanets using a coronagraph requires a telescope/coronagraph system that produces a 10^{-10} contrast dark-hole with as small of an inner working angle (IWA) as possible and as large of an irradiance throughput as possible. The smaller the IWA and the larger the throughput, the greater the number of habitable zones that can be searched. The ability to achieve a small IWA depends upon the telescope's ability to produce a small stable point spread function (PSF). The smaller the PSF, the smaller the IWA. It is common knowledge that the larger a telescope's aperture, the smaller its PSF. But, what is often overlooked is that an unobscured (off-axis) telescope always has a smaller PSF than an on-axis telescope – because diffraction from the central obscuration broadens the PSF. To be specific, an unobscured circular aperture has 82.8% encircled energy (EE) at λ/D. And, a telescope with a 10% central obscuration, has 82.5% EE at 1.4 λ/D. And, for a 20% obscuration, the 82% EE is at 1.63 λ/D).[3] Thus to achieve the same IWA as an unobscured 4-m telescope, a 10% central obscuration telescope needs to be 5.6-m and a 20% obscured telescopes needs to be 6.5-m. Additionally, diffraction from secondary mirror spider obscurations distort the PSF and broaden the EE. A 1 to 2% wide spider can increase EE diameter (IWA) by 5 to 10%[3] – requiring a 5 to 10% larger on-axis telescope. Of course the problem is even worse for a segmented aperture primary mirror. Figure 1 shows the core throughput for three different coronagraphs: vector-vortex charge 4 (VVC4), vector-vortex charge 6 (VVC6) and hybrid Lyot (HLC) with the HabEx baseline 4-meter off-axis unobscured telescope; and, the throughput for a 6-m on-axis segmented primary mirror telescope (i.e. JWST) with an apodized pupil Lyot coronagraph (APLC).[4]

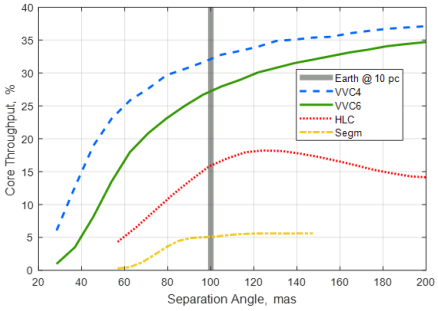

Figure 1: Core throughput versus separation angle. Vertical line is Exo-Earth at 10 pc (100 mas).[5]

Regarding minimum aperture and diffraction limit, the specification is based on a design reference mission yield estimate for an off-axis-telescope/coronagraph combination.[5] Threshold science occurs when the telescope PSF core radius (λ/D) is 20 mas. This is accomplished with a 4-m off-axis monolithic aperture telescope with a 400 nm diffraction limit.

2.2 Telescope Wavefront and Primary Mirror Surface Specification

The science requirement for a 400 nm diffraction limited performance telescope drives the total primary mirror (PM) surface specification – particularly the low-spatial frequency portion of that specification. The exoplanet science high-contrast imaging requirement drives the mid- and high-spatial frequency portion of the PM specification.

To have a 400 nm diffraction limited performance (Strehl ratio ~ 80%) telescope requires a total system wavefront error (WFE) of approximately 30 nm rms. Contributors to a telescope total system WFE are the primary mirror (PM), secondary mirror (SM) and tertiary mirror's (TM) surface figure errors, and the ability to attached the PM and SM to the structure and accurately align them to the TM and maintain that alignment on-orbit (Figure 2). Please note that, because the telescope has a laser metrology system that establishes and maintains PM and SM alignment to the TM with high precision, the majority of the telescope wavefront error budget can be allocated to the mirrors. And, because the PM is larger and less stiff than the SM or PM, it gets the larger allocation.

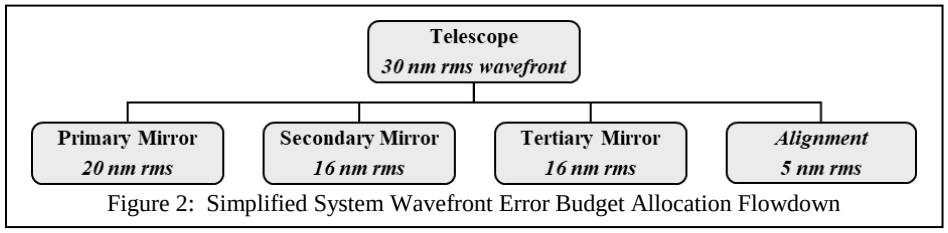

Figure 2: Simplified System Wavefront Error Budget Allocation Flowdown

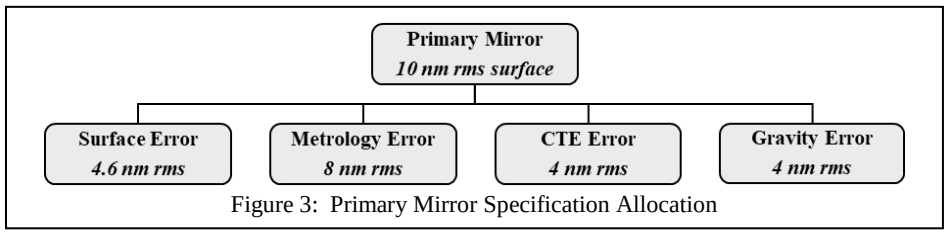

Figure 3: Primary Mirror Specification Allocation

Figure 3 shows how the PM WFE allocation flows into a nominal primary mirror engineering specifications. The reader is reminded that surface error is half of wavefront error and that these specifications are independent of aperture size. This error budget defines the engineering specifications which must be achieved by the PM fabrication process. Surface figure error allocation is set to what is demonstrated on WFIRST.[6] Metrology error is set to what was demonstrated on JWST.[7] The last two boxes define the specific technology challenges that require maturation: ability to quantify PM CTE homogeneity and ability to quantify and removed gravity sag from the PM surface shape, i.e. produce a '0-G' mirror.

2.2.1 Primary Mirror Surface Figure Error

As previously discussed, Exoplanet science wants to image planets in the Habitable Zone. But, for terrestrial mass planets in the HZ around G-type stars (e.g., the Sun), the ratio of reflected planet light to emitted starlight is ~10^{-10}. Thus, it is necessary to 'block' the light from the star in order to 'see' the planet. This is accomplished in a coronagraph. For a 'perfect' telescope, it is possible to create a mask to block the PSF produced by the star and pass the PSF of the planet. But, in a 'real' telescope, wavefront errors redistribute the light making it impossible to create the required 10^{-10} contrast. Mid-spatial frequency errors blur or spread the core. And high-spatial frequency errors and surface roughness scatter light out of the core and over the entire PSF. Thus, while General Astrophysics science is most interested in the shape and stability of the PSF, Exoplanet science is particularly interested in mid- and high-spatial frequency errors that move light from the host star out of the core and masks the light from the planet. Thus, per Table 2, the total PM surface figure specification is further divided into low-, mid- and high-spatial frequency bands.

Table 2: HabEx Primary Mirror Surface Figure Error Specification

	Surface	Wavefront
Total Error	< 4.6 nm rms	< 9.2 nm rms
Low Spatial SFE (< 7 cycles/diameter)	< 3.5 nm rms	< 7.0 nm rms
Mid Spatial SFE (7 to 100 cycles/diameter)	< 3.0 nm rms	< 6.0 nm rms
High Spatial SFE (> 100 cycles/diameter)	< 0.4 nm rms	< 0.8 nm rms
Roughness	< 0.07 nm rms	< 0.14 nm rms

Please note that the boundary between low and mid-spatial is somewhat arbitrary. It assumes that the fabrication process up to 7-cycles is deterministic (i.e. computer controlled) and above 7-cycles is stochastic or random. The 100-cycle boundary between mid and high spatial has an engineering basis. Coronagraphs use deformable mirrors (DM) to create a 'dark hole' by correcting low-spatial frequency errors and moving light from the hole zone back into the core. A 64×64 DM can theoretically correct spatial frequencies up to 32 cycles (or half the number of DM elements). This could create a 'dark hole' with an inner working angle (IWA) of λ/D and an outer working angle (OWA) of $32\lambda/D$. The problem is that primary mirror spatial frequency errors up to 3X beyond what can be corrected by the DM can scatter energy back into the 'dark hole'. Therefore, the primary mirror needs have a surface figure < 4 nm rms for spatial frequency errors from 30 cycles up to 100 cycles[8-9].

2.2.2 Primary Mirror Coefficient of Thermal Expansion (CTE) Error

CTE error is important because it can introduce low and mid-spatial frequency surface figure error. CTE error has two components. First is knowledge of the exact temperature at which the mirror's CTE is zero. Any operational departure from this temperature will introduce a wavefront error – primarily power. Fortunately, this error can be mitigated by adjusting the on-orbit operating temperature for a minimum WFE. The second, and more important error, is mid-spatial frequency residual cryo-null-polishing error. Because of CTE inhomogeneity in the mirror substrate, the mirror will have a different shape at its operating temperature than at its manufacture temperature. This is a particular problem for cryogenic telescopes and is mitigated via cryo-null-figuring (CNF). For example the JWST mirror segments, which operate at 30K (270K below their manufacture temperature), had to be CNF'ed for many 10s of nanometers of cryo-deformation.[7] HabEx requires CNF because it has an extremely smooth surface figure error specification and it plans to operate at a nominal temperature of 270K (i.e. 30K below its likely fabrication temperature). The exact amount of WFE that must be CNFed depends on the mirror substrate's CTE homogeneity. For example, Figure 4 shows a 1.2-m extreme-lightweight Zerodur® (ELZM) mirror with a 9.8-nm rms cryo-deformation over a 62K temperature range. Analysis indicates that this mirror has a CTE homogeneity of +/- 5-ppb/K.[10] Of course, this error could be corrected via a deformable mirror, but it is better for the primary mirror to have good CTE homogeneity. Therefore, a non-destructive process to quantify CTE homogeneity of a 4-m mirror substrate with a spatial sampling of at least 100 x 100 to better than +/- 1 ppb/K is an enabling technology to be demonstrated.

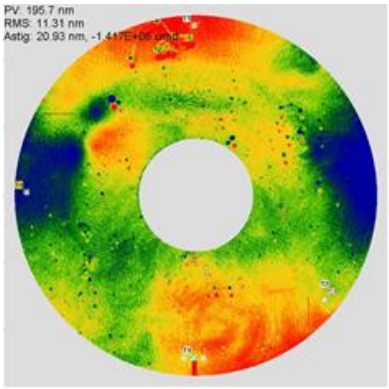

Measured Delta-SFE 292-230K

Index N	Index M	Zernike Term	TOTAL RMS 9.76 nm rms
1	1	Tilt	0.05
2	0	Power	0.24
2	2	Astig	8.55
3	1	Coma	0.90
4	0	Spherical	0.27
3	3	Trefoil	2.15
4	2	Secondary Astig	0.72
5	1	Secondary Coma	0.75
6	0	Secondary Spherical	0.40
4	4	Tetrafoil	1.73
5	3	Secondary Trefoil	1.39
6	2	Tertiary Astig	0.93
7	1	Tertiary Coma	0.77
8	0	Tertiary Spherical	0.24
5	5	Pentafoil	0.53
6	4	Secondary Tetrafoil	0.29
7	3	Tertiary Trefoil	1.72
8	2	Quaternary Astig	0.04
9	1	Quaternary Coma	0.81
10	0	Quaternary Spherical	0.57
6	6	Hexafoil	1.28
7	5	Secondary Pentafoil	0.49
8	4	Tertiary Tetrafoil	0.48
9	3	Quaternary Trefoil	1.20
10	2	Quinary Astig	0.58
11	1	Quinary Coma	0.45
12	0	Quinary Spherical	0.75

Figure 4: 1.2m Schott ELZM 62K thermal deformation.

2.2.4 Primary Mirror Gravity Sag Figure Error

Gravity sag error occurs because space mirrors are manufactured in a 1-G environment. During fabrication, mirrors experience self-weight deflection when attached to their metrology mount. But in the 0-G environment of space, there is no self-weight deflection. The deformation in the mirror's shape from 1-G to 0-G is called G-release.

Gravity sag consists of two components: self-weight mount deflection and facesheet deflection. Self-weight mount deflection occurs due to the reaction or bending of the mirror substrate as it is accelerated by gravity against its opto-mechanical support mount. Facesheet deflection occurs because space mirrors are typically lightweighted – leaving parts of the facesheet without support. These parts deflect due to the acceleration of gravity against the vertical core ribs. For the purposes of this paper, we will ignore facesheet deflection because facesheet gravity deflection is typically a smaller effect than fabrication quilting. The reason is that force exerted onto the facesheet by grinding and polishing is typically greater than that of gravity. Also, methods to mitigate facesheet deflection and quilting at the scale of HabEx's 4-m mirror are TRL-9. One proven mitigation approach is to design the mirror with an appropriately thick facesheet and core pocket dimensions. Another approach is to pressurize the mirror core cells to balance gravity during the fabrication process.

To produce a diffraction limited space telescope, the primary mirror must be fabricated to its required on-orbit 0-G figure. For HabEx, the desired G-release error is < 4 nm rms. Of course, this error could be corrected via a deformable mirror, but it is better for the primary mirror to have good '0-G' figure. Therefore, a validated process to quantify over a 100 × 100 spatial sampling of the self-weight gravity deflection of a nominal 80-Hz first mode 4-m class space-flight mirror on its flight-mount to an uncertainty of bettern that 4 nm rms is an enabling technology to be demonstrated.

2.2 Wavefront Error (WFE) Stability Specification

WFE stability specification is driven by the coronagraph. Any temporal or dynamic change in WFE can result in dark-hole speckles that produce a false exoplanet measurement or mask a true signal. The engineering issue is how large of a WFE can a coronagraph tolerate. Currently, HabEx is baselining a Vector Vortex Coronagraph charge 6 (VVC-6) where 'charge' indicates the coronagraph's azimuthal shear. The higher the 'charge' the more low order error it can tolerate, but the larger its IWA and the lower its throughput. A VVC-4 tolerates tilt and focus error while a VVC-6 tolerates astigmatism, coma and spherical.

WFE instability can arise from many sources – mechanical and thermal – but the primary sources are LOS Jitter, Inertial motion and Thermal drift. LOS jitter produces WFE instability due to beam-shear on the secondary and tertiary mirrors. Because the mirrors are conics, beam shear manifests itself as low-order astigmatism and coma (shear of spherical aberration is coma and sub-aperture coma appears to be astigmatism). Inertial WFE instability occurs when the primary mirror is accelerated by mechanical disturbances causing it to react (i.e. bend) against its mounts (Figure 5). The shape of the inertial WFE instability can be tailored by adjusting the geometry of the mirror mount design, i.e. 3 vs 6 vs 9-point mount, and location of mounts, i.e. edge vs 70% radius.[11-13]

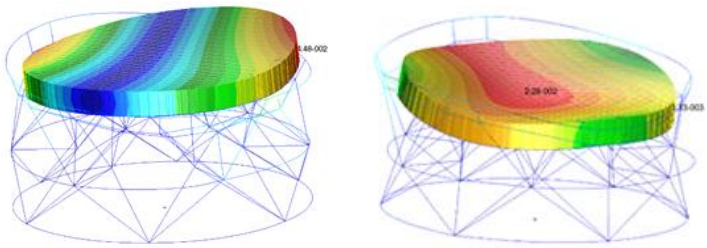

Figure 5: Mirror bends when it reacts against its mount caused by rocking or bouncing modes.

Thermal WFE instability occurs when the primary mirror's bulk temperature or temperature gradient changes. If the mirror's coefficient of thermal expansion (CTE) is completely homogeneous and constant, then a bulk temperature should only result is a defocus error. But any inhomogeneity in the mirror's CTE causes a temperature dependent WFE. Additionally, because CTE is itself temperature dependent, any change in the mirror's thermal gradient also causes a WFE. Please note that unlike mechanical WFE which is mostly low-spatial-frequency, thermal WFE can have significant high-spatial-frequency content. For example, the mirror in Figure 4 has 2.2 nm rms of trefoil, 1.7 nm rms of tetrafoil and 1.3 nm rms of hexafoil. Thus, if a 60K thermal change produces 5-nm rms of trefoil wavefront and the error budget tolerance is 0.5-pm rms, then the mirror needs to be kept thermally stable to 6-mK. But, if the mirror's CTE homogeneity only produces 2.5 nm rms of trefoil, then it need only be kept thermally stable to 12-mK.

Therefore, CTE homogeneity drives the mirror's required thermal stability. And, a non-destructive process to quantify CTE homogeneity of a 4-m mirror substrate with a spatial sampling of at least 100 x 100 to better than +/- 1 ppb/K is an enabling technology to be demonstrated.

Additionally, thermal environment changes can also produce LOS drift – because of structure CTE – but because such drift is slow, the baseline telescope's laser alignment metrology system can sense and correct for this drift. As with LOS jitter being a structure challenge solved by micro-thruster technology, Thermal LOS drift is a structure challenge solved by laser metrology technology. Therefore, it will not be discussed further in this paper.

A wavefront stability error budget for the HabEx baseline telescope (Table 3) was developed using performance predicted by an integrated observatory structural thermal opto-mechanical performance (STOP) model.[14] The first set of columns lists the Zernike polynomial indices and common names. The next set of columns are the predicted STOP performance for each error source. (Please note that each prediction contains a modeling uncertainty factor of 2 to 4X.) These predictions are RSSed to yield a total RMS WFE for each Zernike term. The final column is the allowed telescope WFE stability tolerance calculated using the Noise Equivalent Contrast Ratio (NECR) method[4] to distribute errors between terms to provide a uniform 2X margin between predicted performance and allowed error budget tolerance. While astigmatism has the largest tolerance, it is unimportant because the VVC-6 is insensitive to astigmatism. Instead, the most important term in the error budget is trefoil. Please note that this error budget is ONLY for the baseline Zerodur primary mirror. The error budget will be different for a different mirror substrate or mount design.

Table 3: Telescope Wavefront Error Stability Error Budget

Index			Predicted WFE Performance [pm rms]			Total Predicted WFE	WFE Tolerance
N	M	Aberration	Jitter	Inertial	Thermal	[pm rms]	[pm RMS]
		TOTAL RMS	1.767	3.994	5.565	7.074	14.576
1	1	Tilt	0.681	0.123	0.026	0.693	1.427
2	0	Power (Defocus)	1.208	1.430	3.759	4.199	8.653
2	2	Astigmatism	1.069	3.559	3.463	5.080	10.466
3	1	Coma	0.240	0.099	0.345	0.432	0.889
4	0	Spherical	0.004	0.213	0.405	0.458	0.943

3	3	Trefoil	0.012	1.039	2.098	2.341	4.824
4	2	Sec Astigmatism	0.004	0.178	0.108	0.208	0.429
5	1	Sec Coma	0.001	0.026	0.105	0.108	0.223
6	0	Sec Spherical	0.000	0.028	0.000	0.028	0.058
4	4	Tetrafoil	0.000	0.198	0.189	0.274	0.564
5	3	Sec Trefoil	0.000	0.112	0.233	0.259	0.533
6	2	Ter Astigmatism	0.000	0.021	0.000	0.021	0.043
7	1	Ter Coma	0.000	0.033	0.000	0.033	0.068
5	5	Pentafoil	0.000	0.074	0.217	0.229	0.472
6	4	Sec Tetrafoil	0.000	0.029	0.000	0.029	0.060
7	3	Ter Trefoil	0.000	0.015	0.000	0.015	0.031
6	6	Hexafoil	0.000	0.026	0.000	0.026	0.054
7	5	Sec Pentafoil	0.000	0.015	0.000	0.015	0.031
7	7	Septafoil	0.000	0.010	0.000	0.010	0.021

3. HABEX TELESCOPE AND PRIMARY MIRROR DESIGN

3.1 Baseline HabEx Optical Telescope

The 'baseline' telescope (Figure 6) consists of the primary mirror assembly, secondary mirror assembly, secondary mirror tower with integrated science instrument module, and stray-light tube with forward scarf. The scarf determines the closest angle of observation to the sun. The tower and tube are the optical bench that maintains alignment between the PMA, SMA and TMA. The OTA is physically separate from the spacecraft – connecting only at the interface ring. This ring is also the interface between the payload and the Space Launch System. Instead of reaction wheels, thrusters slew the observatory and micro-thrusters provide fine pointing control.

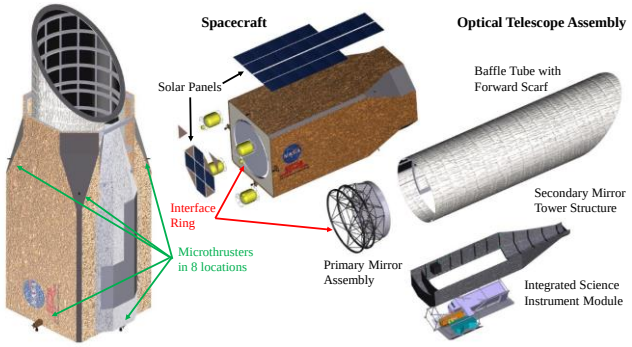

Figure 6: Baseline HabEx Observatory Payload

3.2 Baseline HabEx Primary Mirror Assembly

The baseline Zerodur® mirror is designed to balance mass and stiffness. Stiffness is important because it enables performance and simplifies manufacture. The higher a mirror's stiffness, the easier (less expensive and shorter schedule) it is to produce the smooth surface needed to achieve 400 nm diffraction limited performance. The easier it is to handle (i.e. mount to machinery or simply turning over), which reduces fabrication risk. And, the smaller will be its inertial wavefront error and the less likely it is that the mirror will have significant G-release error – both of which are related to gravity sag or self-weight deflection. Mass is important because it provides thermal capacity for a thermally stable mirror.

The baseline Zerodur® mirror has a flat-back geometry with a 42 cm edge thickness and mass of approximately 1400 kg. (Figure 7) The mirror's free-free first mode frequency is 88 Hz. And, its mounted first mode frequency is 70 Hz. The mirror is locally stiffened to minimize gravity sag.[12] The substrate geometry and mount designs were optimized to produce as uniform as possible XYZ gravity sag deformation. The mirror is attached at three edge locations to a hexapod mount system. This geometry was selected to allow defocus and minimize spherical gravity sag based on vector vortex coronagraph aberration sensitivity. Figure 8 shows the baseline mirror's predicted 1-G PV surface gravity sag in global telescope XYZ coordinate system.

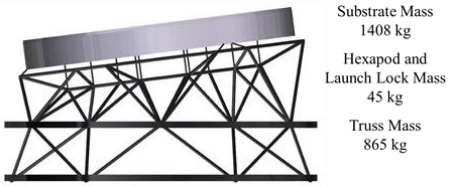

Figure 7: Primary Mirror Assembly

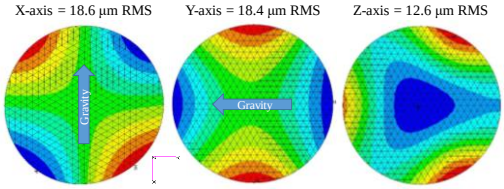

Figure 8: Primary Mirror Gravity Sag (surface)

4. TECHNOLOGY READINESS LEVEL (TRL) ASSESSMENT

According to NASA NRP 7123, all technologies for a proposed mission must be TRL-5 for the start of Preliminary Design Analysis (Phase-A) and TRL-6 by Preliminary Design Review (PDR) and the start of final design and Fabrication (Phase-C). TRL definitions are summarized in Figure 9.

TRL	Definition	Description	Exit Criteria
1	Basic principles observed and reported	Scientific knowledge generated underpinning hardware technology concepts/applications	Peer reviewed publication of research underlying the proposed concept/application
2	Technology concept and/or application formulated	Invention begins, practical application is identified but is speculative, no experimental proof or detailed analysis is available to support the conjecture	Documented description of the application/concept that addresses feasibility and benefit
3	Analytical and experimental critical function and/or characteristic proof of concept	Analytical studies place the technology in an appropriate context and laboratory demonstrations, modeling and simulation validate analytical prediction	Documented analytical/experimental results validating predictions of key parameters
4	Component and/or breadboard validation in laboratory environment	A low fidelity system/component breadboard is built and operated to demonstrate basic functionality and critical test environments, and associated performance predictions are defined relative to the final operating environment	Documented test performance demonstrating agreement with analytical predictions. Documented definition of relevant environment
5	Component and/or breadboard validation in relevant environment	A medium fidelity system/component brassboard is built and operated to demonstrate overall performance in a simulated operational environment with realistic support elements that demonstrates overall performance in critical areas. Performance predictions are made for subsequent development phases	Documented test performance demonstrating agreement with analytical predictions. Documented definition of scaling requirements
6	System/sub-system model or prototype demonstration in an operational environment	A high fidelity system/component prototype that adequately addresses all critical scaling issues is built and operated in a relevant environment to demonstrate operations under critical environmental conditions	Documented test performance demonstrating agreement with analytical predictions
7	System prototype demonstration in an operational environment	A high fidelity engineering unit that adequately addresses all critical scaling issues is built and operated in a relevant environment to demonstrate performance in the actual operational environment and platform (ground, airborne, or space)	Documented test performance demonstrating agreement with analytical predictions
8	Actual system completed and "flight qualified" through test and demonstration	The final product in its final configuration is successfully demonstrated through test and analysis for its intended operational environment and platform (ground, airborne, or space)	Documented test performance verifying analytical predictions
9	Actual system flight proven through successful mission operations	The final product is successfully operated in an actual mission	Documented mission operational results

Figure 9: TRL Definitions from NASA.

As summarized in Figure 10, all but three of the technologies needed to manufacture a potential HabEx primary mirror are assessed to be at TRL-6. The remaining are assessed to be at TRL-4. As discussed in Section 2.0, the issues driving the ability to achieve the required surface figure error for diffraction-limited performance and for achieving the required wavefront stability are mirror substrate CTE homogeneity and gravity sag. Therefore, the technologies which need to be demonstrated in order to assess the ability to make a 4-m 80-Hz primary mirror to be TRL-6 are: 1) a non-destructive process to quantify CTE homogeneity of a 4-m mirror substrate with a spatial sampling of at least 100 x 100 to better than +/- 1 ppb/K; and, 2) a process to quantify self-weight gravity deflection to better than 4-nm rms over a 100 x 100 spatial sampling. Section 5.0 defines a roadmap to mature these technologies, with modest investment, to TRL-5 by 2024. Independently, under existing Astrophysics Division directed work funding, the Predictive Thermal Control project is maturing thermal control technology needed to achieve the required wavefront stability.[15]

Large Mirror Fabrication			
Technology	**Need**	**State of the Art**	**TRL**
Mirror Substrate Diameter	4.04 meter	Schott Corp manufactures blanks that are 4.2 m diameter x 420 mm thick	6
Mirror Substrate CTE			
• Bulk CTE	0 at 270 K	Schott Corp can tune CTE to be 0 at a specific temperature.	6
• CTE Homogeneity	< +/- 5 ppb/K over 100 x 100 spatial sampling	Schott Corp demonstrated < +/- 3 ppb/K over limited spatial sampling on DKIST	4
Substrate Machining	3–4 mm ribs, 14 mm facesheet, and pocket depth of 290 mm for 400 mm thick blank	Schott Corp demonstrated computer-controlled-machine lightweighting to pocket depth of 340 mm, 4 mm rib thickness on E-ELT M5 and 240 mm deep/2 mm thick rib on Schott 700 mm diameter test unit	6
Areal Density	110 kg.m^2	State-of-the-practice lightweighting has made large glass mirrors with aerial density of 70 kg/m^2	6
First Mode Frequency	≥ 60 Hz	By design, if the baseline Zerodur® mirror substrate can be machined to its specified dimensions using demonstrated Schott Corp machining capability, it will achieve the required first mode frequency. Also, sub-scale WFIRST 2.4-m Primary Mirror has ~ 200 Hz first mode.	6
Wavefront Error	0-7 cy/D: 6.9 nm RMS 7-100 cy/D: 6.0 nm RMS >100 cy/D: 0.8 nm RMS	Demonstrated on sub-scale WFIRST 2.4-m Primary Mirror	4
Wavefront Stability	1 to 100 pm rms	By design, baseline Zerodur® mirror will achieve required wavefront stability with active zonal thermal control stability of < 5-mK. Sub-scale active thermal control has been demonstrated by Harris Corp to TRL-9 on 1.1-m Spaceview™	4

Figure 10: HabEx Large Mirror Fabrication TRL Assessment.

4.1 TRL Assessment of 4-meter Mirror Substrates

As 'zero' CTE materials, both Zerodur® and ULE® were considered for the primary mirror. Both are TRL-9. ULE® mirror systems flying in space include: Hubble's 2.4-m mirror, Kepler's 1.4-m mirror, and the WorldView commercial imaging system's 1.1-m mirrors. Zerodur® has flown over 30 systems, the largest of which are the 0.8-m 73% lightweighted METEOSATs.[16] Zerodur® was selected because Schott's ability to make a 4-m mirror substrate is assessed to be TRL-6 while Corning's ability to fabricate a 4-m mirror substrate is assessed to be TRL-5.

Schott routinely casts 4.2 meter diameter x 42 cm thick mirror blanks of ultra-homogeneity CTE Zerodur® and machines them into 2-m x 1-m x 40-cm thick lightweight ultra-stiff structures for its lithography bench product line.[17] Recent examples of 4-m mirrors made from such blanks are the Daniel K. Inouye Solar Telescope (DKIST) primary mirror and the European Extremely Large Telescope (E-ELT) secondary mirror (Figure 11).

Using its 5-m 5-axis computer-numerically-controlled (CNC) machining center (Figure 12), Schott routinely machines these 4-m blanks into 2-m x 1-m x 40-cm thick lightweight ultra-stiff structures (for its lithography bench product line) with ribs as thin as 2 mm (Figure 13).

Figure 11: DKIST 4-m primary mirror (top); E-ELT 4-m secondary mirror (bottom).

Figure 12: Schott 5-m 5-axis CNC Machining Center.

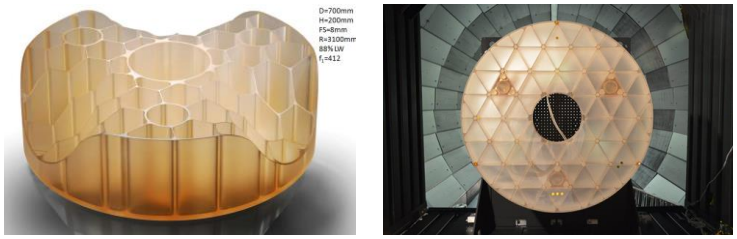

Figure 13: 0.7-m dia 200-mm thick mirror with 2-mm ribs (left); 1.2-m dia 125-mm thick mirror with 2-mm ribs (right).

By comparison, ULE® lightweight space-mirror substrates are assembled by frit-bonding or low-temperature-fusing together mirror facesheets and core elements manufactured from 1.4-m to 1.8-m roundals.[18] And, while Corning has a 4-m class furnace, the largest ULE® mirror manufactured to date is 2.4-meters.

4.2 TRL Assessment of 4-meter Mirror Surface Figure

The ability to polish a 4-m mirror substrate to the HabEx primary mirror surface error specification is assessed to be TRL-6 except for the ability to characterize CTE homogeneity and gravity sag. Multiple organizations have existing infrastructure to grind and polish 4-m class mirrors, including: Collins Aerospace[19], L3/Brashears, L3/Harris, Arizona Optical Systems, University of Arizona, and REOSC. And, all of these have demonstrated the ability to polish space mirrors to a total surface figure error of less than 6 nm rms. Additionally, the HabEx PM surface specification is defined to be the same as the WFIRST PM's current surface figure.

4.3 TRL Assessment of 4-meter Mirror CTE Homogeneity Characterization

The ability to quantify CTE of ULE® and Zerodur® is TRL-9. Corning has demonstrated a non-destructive interferometric process for quantifying ULE® CTE to ~0.1-ppb/K by correlating measured index of refraction variation with CTE variation.[20] The spatial resolution of this process is defined by the interferometer. Schott has demonstrated a dilatometer process that can measured CTE of Zerodur® test samples with a reproducibility of ~ +/- 1 ppb/K.[21] But the problem with the Schott process is that it operates on test samples, it is destructive. Thus, a non-destructive process for evaluating Zerodur® CTE to < 1 ppb/K at spatial resolution of greater than 100 x 100 is required.

Per Table 4, since 2009 Schott has produced seven 4-m mirror substrates with CTE homogeneity less than 10 ppb/K. And one with 3 ppb/K.[21]

Table 4: Schott 4-meter mirror CTE production history.

	Dimension	Number of Samples	CTE (0°; 50°) absolute value [ppb / K]		CTE (0°; 50°) homogeneity [ppb / K]	
Year	[mm]	#	Specification	Achieved	Specification	Achieved
2003	4100 x 171	18	+/- 50	66	20	18[1]
2005	3610 x 370	12	+/- 100	80	30	25[1]
2009	3700 x 163	36	+/- 150	54	40	9
2010	3400 x 180	12	+/- 100	42	30	5
2012	4250 x 350	16	+/- 30	60	40	5
2014	4250 x 350	16	+/- 30	0	40	3
2016	4060 x 103	16	+/- 50	36	20	7
2016	4000 x 100	12	+/- 150	15	20	4
2019	4250 x 100	20	+/- 20*	-9*	20*	8*

But, as listed in Table 4 and shown in Figure 14, the samples used to characterize the CTE of these blanks were taken from a limited number of locations around the outer and inner perimeter of the mirror blanks.[21]

Schott has mapped the 3D CTE homogeneity of meter class blanks via destructive sampling (Figure 15),[21] but this mapping has not been correlated with a non-destructive testing technique such as interferometric characterization of cryogenic surface figure deformation.

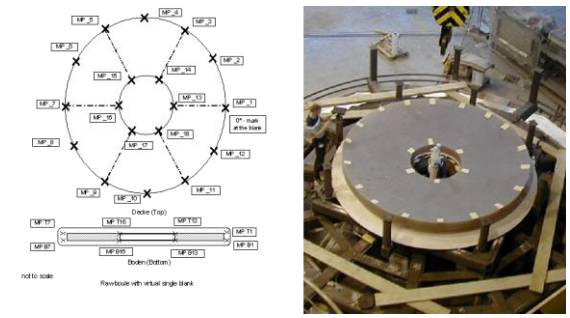

Figure 14: CTE Sample Locations for 4-m Mirror.

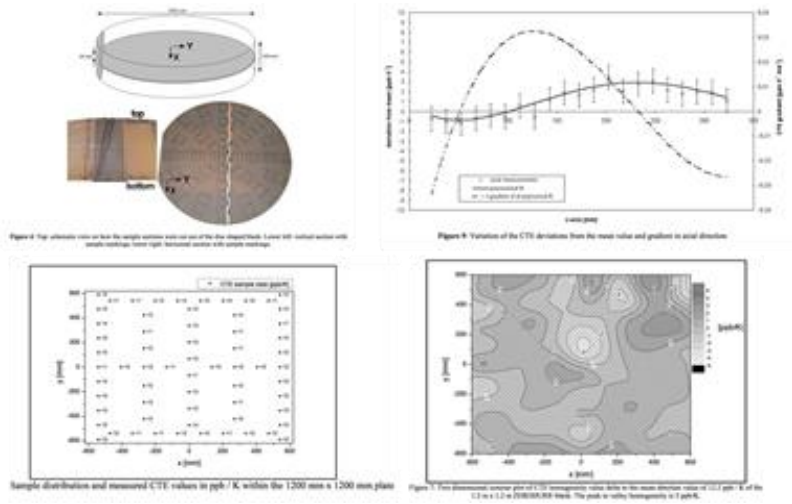

Figure 15: 3D CTE Mapping ins 1.2 meter Zerodur® blanks.

4.4 TRL Assessment of 4-meter Mirror Gravity Sag Characterization

The causes of gravity-sag, its characterization and mitigation have been studied extensively since the 1960s. Thus, there are multiple approaches to mitigate G-release error for HabEx:

- Minimize gravity sag by making the mirror as stiff as possible and optimizing its mounting.
- Off-load gravity during fabrication and test
- Analytically remove gravity sag during tests
- Actively correct mirror shape on-orbit

4.4.1 Make the Mirror Stiff

For any given mirror, self-weight mount deflection gravity sag is proportional to geometry, mass and mount interface.

$$1G\ Gravity\ Sag \sim C_{SP}\left(\frac{D^4}{t^3}\right)\rho_{AD} \sim 1/(2\pi\ f)^2,$$

where C_{SP} is mount support configuration constant[13] (Figure 16), D is mirror substrate diameter, t is mirror substrate thickness, ρ_{AD} is mirror substrate mass areal density, and f is mirror substrate first mode frequency. To minimize gravity sag of a given diameter mirror, make the mirror as thick as possible with as low an areal density as possible. A complete discussion of mirror design methodology can be found in Yoder and Vukobratovich.[13]

Support Constant	C_{SP}	Factor of Reduced Deflection Compared to 3-Pt Support
Ring at 68% of Diameter	0.028	11
6 Points Equal Spaced at 68.1% of Diameter	0.041	8
Edge Clamped	0.187	1.5
3 Points, Equal Spaced at 64.5% of Diameter	0.316	-
3 Points, Equal Spaced at 66.7% of Diameter	0.323	~1
3 Points, Equal Spaced at 70.7% of Diameter	0.359	0.9
Edge Simply Supported	0.828	1/3
Continuous Support along the Diameter	0.943	1/3
"Central Support" (Mushroom or Stalk Mount; r = radius of stalk)	1.206	1/4
3 Points Equal Spaced at Edge	1.356	1/4

Figure 16: Mirror support configuration constants relative to 3-point mount.

At the 4-meter size, it is impossible to make a mirror sufficiently stiff that its G-sag is < 4 nm rms. However, the baseline HabEx Zerodur® mirror is designed to minimize its gravity sag. At 42 cm, the mirror is the maximum thickness that Schott can cast. Edge mounting at 3-points reduces gravity sag. And, the mirror design has an optimized non-uniform areal density to provide localized stiffness that further reduces gravity deformation.

4.4.2 Off-load gravity during fabrication and test

There are two methods to mitigate Gravity-sag during primary mirror fabrication and test, and both are TRL-9: multipoint mount and air bag. For mid-quality mirrors, air bags are adequate. But for high-precision mirrors, multi-point mounts are preferred. The reason is that discrete mount points are more deterministic than a bag surface. Support points can be placed in a known orientation, i.e. perpendicular, to the mirror structure. And, they can be instrumented with force sensors to apply a precisely known upward force at each point.

Multi-point mount technology was developed with NASA funding in the 1970s for the Large Space Telescope Program (Hubble).[13, 22-23] The Hubble primary mirror's 7.6 micrometer PV self-weight deflection was characterized to an accuracy of 1.4 nm rms using a 135 point metrology mount (Figure 17).[13, 24-26] The Kepler primary mirror was tested using both an air bag and a 108 point metrology mount. The air bag was estimated to off-load gravity sag with an uncertainty of 5.6 nm rms. And the difference between the air bag test and multi-point mount test was 16.4 nm rms (mostly spherical aberration).[27] Extrapolating the Hubble mount to the baseline HabEx primary mirror, it may be possible to quantify the ~30 micrometer PV 'face-up' gravity sag of a 4-m 80-Hz mirror to an uncertainty of ~6 nm rms. However, because the baseline HabEx mirror is less stiff than the Hubble mirror, a HabEx mount may require a denser arrangement of support points.

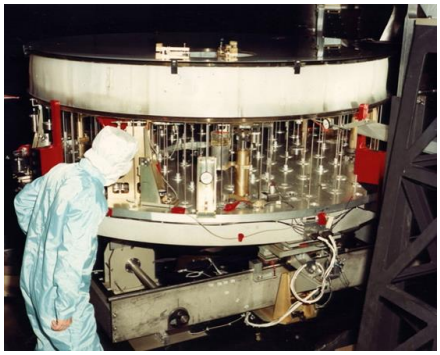

Figure 17: Hubble 135 point metrology mount.

4.4.3 Analytically remove gravity sag during tests

There are two methods to characterize gravity-sag by test and analytically remove it during primary mirror fabrication, and both are TRL-9: vertical face-up/face-down test[27] and the horizontal rotation testing.[18, 28-29] Rotation tests were originally developed to enable the optical precision needed to fabricate optical surfaces for the microlithography industry. Because interferometry is a relative measurement, the ability to manufacture precision surfaces was limited by the knowledge of the reference wavefront (and systematic interferometer errors). The purpose of the absolute calibration tests was to 'calibrate' the reference wavefront against a known surface. This calibrated wavefront could then be subtracted from any interferometer measurement to give a 'better' estimate of the surface under test.

With the advent of digital phase-measuring interferometry, the Evans and Kestner 'N-rotation' algorithm was easy to implement. The interferometer measures a surface at N-rotation angles, i.e. N=3 (0°, 120°, 240°) or N=6 (0°, 60°, 120°, 180°, 240°, 300°). Averaging the measurements removes all test errors with angular dependence up to (N-1) Theta; and, all higher angular order errors that are not harmonics of N. So, a N=3 rotation test will remove 2Theta errors (i.e. coma, secondary coma, tertiary coma, etc.; and, astigmatism, secondary astigmatism, tertiary astigmatism, etc.). However, N=3 case cannot remove trefoil. A N=6 rotation test is required to remove error terms up to 5Theta (i.e. trefoil, tetrafoil, and pentafoil). Also, it is important to note that the N-rotation test is 'blind' to rotationally symmetric errors.

The Kepler mirror was tested using a face-up/face-down gravity orientation test then compared with an air-bag test, and with a FEM prediction. The difference between the air bag and face-up/face-down test was 18.4 nm rms. Additionally, the Kepler up/down and rotation estimates of the gravity sag were compared to a FEM prediction of the gravity sag. The FEM predicted a horizontal gravity sag of 660 nm rms and the rotation test matched it to 21 nm rms. Similarly, the Kepler FEM predicted a vertical gravity sag of 170 nm rms and the face-up/face-down test matched it to 13.3 nm rms.[27]

The issue for HabEx is that the Kepler mirror is stiffer than the proposed HabEx mirror, i.e. its horizontal gravity sag is only about 2 fringes (wavefront). By comparison, the baseline HabEx mirror's gravity sag may be as large as 50 micrometers PV (surface) and will produce as many as 160 fringes (wavefront). This is challenging for a typical commercial interferometer. Fortunately, as will be discussed further in Section 5.2, there is a solution. Use a computer generated hologram (CGH) to compensate for the predicted gravity sag by matching the nulling wavefront in each orientation. CGHs are commonly used to test aspheric mirrors with 100s of micrometers of aspheric departure to uncertainties of ~2 nm rms. In fact, JWST mirrors were tested using CGHs. The JWST primary mirror segments had aspheric departures of 100 micrometers and using CGHs, their test results at Tinsley in Richmond CA agreed with their test results at BATC in Boulder CO agreed with their test results at MSFC in Huntsville AL to better than 10 nm rms.[7]

4.4.4 Actively correct mirror shape on-orbit

While techniques exist to characterize self-weight deflection and produce 0-G space mirrors, it is also possible to mitigate the risk of G-release error via an active mirror (e.g. primary, secondary, or deformable flat mirror). Thus, while it is desirable to manufacture the primary mirror with as small of a G-release uncertainty as possible (TRL-9 capability is < 10 nm rms), an active primary mirror can easily correct 50 to 200 nm rms of error. For example, analysis of the alternative ULE® HabEx primary mirror indicates that 15 actuators can reduce low-order (i.e. astigmatic) G-release error by 20×, 25 actuators can reduce G-release error by 40×, and 50 actuators can reduce G-release error by 100× (Figure 18).[30] Please note that active mirror technology is TRL-9. While they were never used – because they were positioned to correct for astigmatism and not spherical – the Hubble PM had 24 actuators to mitigate the risk of astigmatic G-release error.[13] And, the JWST PM has 18 actuators to mitigate the risk of segment radius matching error.

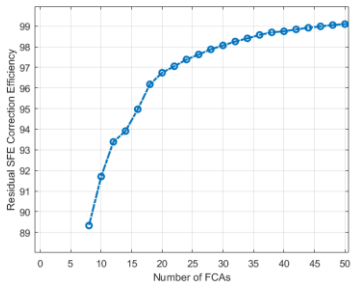

Figure 18: Correctability of alternative ULE® 4-m active primary mirror design as a function of actuators.

5. TECHNOLOGY DEVELOPMENT ROADMAP

TRL 5 would be achieved with a demonstration of thermal stability and surface figure error of a full-scale mirror in a ground support equipment (GSE) mount. A sequence of tests (Figure 19) can minimize cost and risk. A thermal test of the mirror blank, polished to a sphere, would show that the CTE homogeneity requirement over the surface of the mirror is met. Next the blank would be CNC machined for lightweighting, still with a spherical surface polished so that the

gravity sag can be measured; the spherical surface makes optical alignment of the test faster and does not require an additional, custom null corrector element. Then the mirror would be ground to the aspheric prescription and final polishing performed. Note that additional facesheet thickness will be required in the spherical surface of the mirror that will be ground away in the figuring of the aspheric surface. Finally, the surface figure error of the final polished surface is tested and gravity sag backed out. To verify the mechanical stiffness of the mirror, a mechanical ping test will be performed. Shock and vibration are not considered part of the TRL 5 maturity because they are dependent on the mirror assembly, particularly the mirror mount design, and are more appropriately tested at the assembly level for TRL 6.

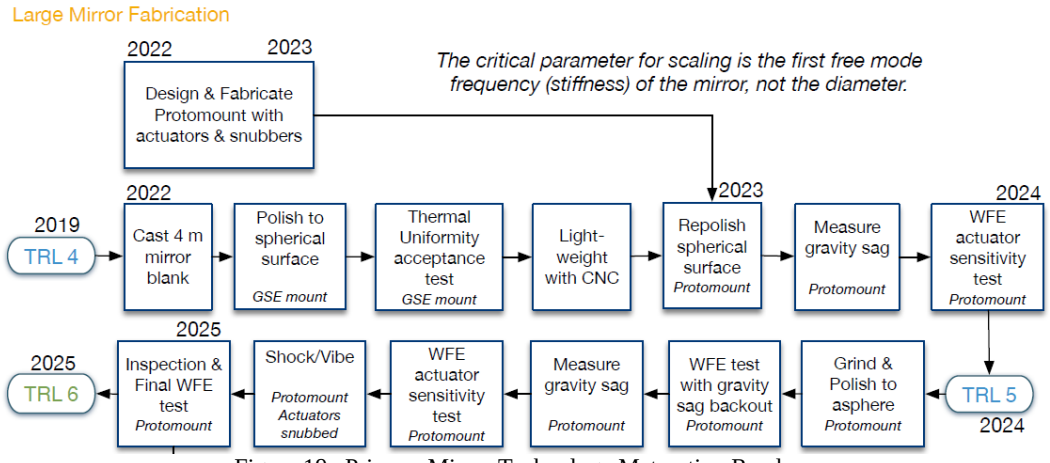

Figure 19. Primary Mirror Technology Maturation Roadmap

5.1 CTE Homogeneity Characterization Process

To perform coronagraphy, HabEx requires a 4-m ultra-thermally stable primary mirror. Analysis indicates that a mirror with CTE homogeneity of better than +/- 5 ppb/K on at least a 100 x 100 spatial scale can achieve the required stability using TRL-9 active thermal control systems.[11] The CTE homogeneity specification is consistent with Schott's demonstrated capability on similar mirror blanks. And of course, the better the mirror's CTE homogeneity, the easier the thermal control stability requirements. The required spatial sampling of least 100 × 100 is driven by dark-hole OWA (outer working angle). Thus, a validated non-destructive process is required to quantify the CTE homogeneity of a 4-m mirror substrate with a spatial sampling of at least 100 x 100 to better than +/- 1 ppb/K.

One potential process to meet this need is to polish a spherical surface into the cast mirror blank and measure its cryo-deformation over a large temperature range, say 60K. The premise is that cryo-deformation is correlated with CTE homogeneity. If the mirror blank were completely homogenous, the only shape change would be power. The purpose of this qualification process is to select a blank for the 4-m HabEx primary mirror based on its CTE homogeneity before undergoing the expensive process of machining it into a lightweight mirror structure.

However, before using this process on a flight mirror, it needs to be demonstrated. And, while such a demonstration might be most convincing if performed on a 4-m substrate, it could also be demonstrated (for lower cost) at a subscale size. To demonstrate a validation process for characterizing CTE homogeneity, the HabEx team proposes the following study:

- Cast two sub-scale blanks and grind/polish spherical surfaces into their fronts.
- Measure the cryo-deformation of each solid mirror over a large temperature range (maybe 60K)
- Cut up one of the mirrors into at least 100 x 100 CTE dilatometer samples
- Measure CTE of each sample with uncertainty < 1 ppb/K
- Correlate measured CTE samples with measured Cryo-Deformation Map
- Machine the second mirror into a lightweight mirror
- Measure the cryo-deformation of 2nd mirror to determine if lightweight machining changes its cryo performance.

5.2 Gravity Deformation Characterization Process

To manufacture a 4-m class 80-Hz first-mode mirror for a 400-nm wavelength diffraction limited performance telescope, a validated process is required to quantify, over a high density 2D sampling, the zero-gravity shape for a flight mirror on

its flight-mount. The required measurement dynamic range is up to 100 micrometers PV driven by the mirror's gravity sag. Required measurement uncertainty is better than 4 nanometers rms driven by deformable mirror range (and ideally 2 nm rms). Required spatial sampling is at least 100 × 100 driven by dark-hole OWA (outer working angle).

To demonstrate a validation process for characterizing and compensating for gravity sag, the HabEx team proposes the following study on the 2nd mirror from the CTE characterization study:

- Predict horizontal and vertical gravity-sag of a test-article mirror assembly using a high-fidelity FEM of the 'as-built' substrate structure and calculated spatial stiffness.
- Makes vertical and horizontal computer generated holograms (CGHs) of the FEM gravity sag predictions.
- Quantify gravity-sag of test-article mirror assembly using N-rotation and face-up/face-down methods.
- Correlate 0-G surface from orientation tests with multi-point mount to calculate up-force needed to off-load gravity at each location of the multipoint mount.

Please note that, to validate this process to TRL-6, it is not necessary to demonstrate the process on a 4-m mirror. Rather, it is only necessary to demonstrate the process on a mirror with a 'representative' first mode stiffness. An 80-Hz mirror at 1.5-m or 2-m will have the same gravity sag as an 80-Hz 4-m mirror.

Making a high-fidelity FEM model to predict gravity sag: Spatial stiffness information allows for one to account for small variations in the mirror's 'as-built' structure. To generate a spatial stiffness map, mount the mirror to a multipoint fabrication/metrology mount. Depending on the size of the mirror, such a mount might consist of 70 to 210 (or more) force-feed-back actuators. Then, 'poke' the mirror at each support point and measure its deformation, i.e. its influence function. Once the mirror's response is known at every point, one can solve for the mirror's local stiffness at each point. With this information, one can calculate the precise up-force needed to off-load gravity at each point. And, one can predict the mirror's deflection in different gravity orientations, i.e. horizontal or vertical. Similar approaches are commonly used on large ground-based telescope mirrors to compensate for gravitational deformation as the telescope slews.

Quantifying gravity-sag via orientation tests: Orientation tests such as the N-rotation test or up/down test are proven methods for quantifying gravity sag. But in the case of HabEx, the self-weight deformation to be measured may be significant (i.e. up to 100 micrometers). Therefore, it is necessary to reduce the influence of this deformation. One potential method is the use of computer generated holograms (CGHs). Using the high-fidelity FEM, predict the mirror assembly's N-rotation test non-rotating gravity-sag and make a CGH of this prediction. This error should be astigmatism. In the N-rotation test there are four components to the mirror-assembly's surface shape. A rotationally symmetric error – to which the test is 'blind'. A rotational error that is part of the mirror's actual shape. A non-rotating error that is caused by the gravity gradient. And, a gravity deformation term that varies with rotation orientation but averages to zero. Testing the mirror with the CGH will generate an estimate of the mirror's asymmetric error (i.e. the component that rotates) and the difference between the mirror's predicted gravity-sag (being cancelled/nulled by the CGH) and the mirror's actual gravity-sag – measured non-rotating component. Because the CGH does not rotate with the mirror, but remains fixed to the interferometer, its errors are common to all measurements and thus irrelevant. Removing the residual gravity-sag term yields an estimate of the mirror's 0-G shape.

Similarly, use the FEM to predict the mirror assembly's face-up and face-down gravity sags and create two complimentary CGHs. If the two CGHs are placed together, when testing a calibration sphere, they should produce no error, i.e. they should cancel each other. But, when used alone to test the mirror face-up or face-down, they will remove their respective terms from the test, leaving only the mirror's surface shape and differences between the predicted complimentary terms and the actual terms. Once the two tests are complete, they are averaged to estimate the 0-G shape of the mirror.

The last step is to correlate the measured residual gravity sag with the FEM to optimize the up-force required to off-load gravity sag at each location of the multipoint mount and to estimate the multipoint mount's off-loading uncertainty.

Finally, as shown in Figure 19, please note that gravity sag characterization occurs while the mirror is a sphere. Aspheric prescription does not contribute to gravity sag. But it does contribute to measurement uncertainty – because of optical axis misalignment. Thus, to reduce measurement uncertainty and schedule risk, the flight mirror's gravity sag on its flight mount will be characterized while the mirror is a sphere. The knowledge of this deformation will be attached to the flight mirror as it is processed into a parabola via fiducials.

6. CONCLUSIONS

The Habitable Exoplanet Observatory mission concept (HabEx) is under study for the 2020 Astrophysics Decadal Survey. Its goal is to image and spectroscopically characterize planetary systems in around nearby sun-like stars. Critical to achieving the HabEx science goals is a large, ultra-stable UV/Optical/Near-IR (UVOIR) telescope. The desired telescope is a 4-meter off-axis unobscured three-mirror-anastigmatic, diffraction limited at 400 nm with wavefront stability on the order of a few 10s of picometers. The baseline HabEx telescope is designed using standard engineering practice and its design 'closes'.

Central to the baseline telescope design is a 4-meter primary mirror with less than 8-nm rms surface figure error and picometer level wavefront stability. The technologies to manufacture and certify such a mirror is assessed to be technology readiness level 6 (TRL-6) for all but two TRL-4 technologies:

- Non-destructive process to quantify CTE homogeneity of a 4-m mirror substrate with a spatial sampling of at least 100 x 100 to better than +/- 1 ppb/K.
- Process to quantify self-weight gravity deflection to better than 4-nm rms over a 100 x 100 spatial sampling.

A technology development roadmap has been defined to mature these two technologies to TRL-6 by 2025.

ACKNOWLEDGEMENTS

This paper is based on work performed under the NASA Astrophysics Division funded HabEx concpt study by the JPL and NASA MSFC HabEx Study Team. MSFC Team: Michael Effinger, Scott Smith, Thomas Brooks, Jacqueline Davis, Brent Knight, Mark Stahl; Willian Arnold (AI Solution); Mike Baysinger, Jay Garcia, Ron Hunt, Andrew Singleton, Mary Caldwell and Melissa Therrell (Jacobs); Bijan Nemati (UAH); and interns Jonathan Gaskin (UNCC), Jonathan McCready (NCSU), and Hao Tang (UoMI). JPL Team: Keith Warfield, Gary Kuan, Stefan Martin, Velibor Cormarkovic, Scott Howe, Juan Villalvazo, Stuart Shaklan, and Team X.

REFERENCES

[1] Committee for a Decadal Survey of Astronomy and Astrophysics; National Research Council, New Worlds, New Horizons in Astronomy and Astrophysics, The National Academies Press, Washington, D.C., 2010.

[2] NASA Space Technology Roadmaps and Priorities: Restoring NASA's Technological Edge and Paving the Way for a New Era in Space, NRC Report, 2012.

[3] Harvey, James E. and Christ Ftaclas, "Diffraction effects of telescopes secondary mirror spiders on various image-quality criteria", Applied Optics, Vol. 34, No. 28, pp-6337, 1 Oct 1995.

[4] Nemati, Bijan, H. Philip Stahl, Mark T. Stahl, and Garreth Ruane "HabEx Telescope WFE stability specification derived from coronagraph starlight leakage", Proc. SPIE 10743, Optical Modeling and Performance Predictions X, 107430G (17 September 2018); doi: 10.1117/12.2312662;

[5] Morgan, Rhonda, et. al., "HabEx yield modeling with for systems engineering", SPIE 10398-3, 2017.

[6] John Krist, Private Communication (June 2019).

[7] Stahl, H. Philip, et. al., "Survey of interferometric techniques used to test JWST optical components", SPIE Proceedings 7790, 2010, DOI:10.1117/12.862234

[8] Shaklan, Green and Palacios, "TPFC Optical Surface Requirements", SPIE 626511-12, 2006.

[9] Shaklan & Green, "Reflectivity and optical surface height requirements in a coronagraph", Applied Optics, 2006

[10] Brooks, Thomas E., Ron Eng, Tony Hull, H. Philip Stahl, "Modeling the Extremely Lightweight Zerodur Mirror (ELZM) thermal soak test", Proc. SPIE 10374, Optical Modeling and Performance Predictions IX, 103740E (6 September 2017); doi: 10.1117/12.2274084

[11] Arnold, William R, H. Phillip Stahl, "Influence of core and hexapod geometry, and local reinforcement on the performance of ultra lightweight ULE mirror," Proc. SPIE 10743, Optical Modeling and Performance Predictions X, 107430B (17 September 2018); doi: 10.1117/12.2326017

[12] Arnold, William R., H. Philip Stahl, "Design trade Study for a 4-meter off-axis primary mirror substrate and mount for the Habitable-zone Exoplanet Direct Imaging Mission", Proc. SPIE 10398, UV/Optical/IR Space Telescopes and Instruments, 1039808 (5 September 2017); doi: 10.1117/12.2275193

[13] Yoder, Paul and Danial Vukobratovich, Opto-Mechanical Systems Design, Fourth Edition, Two Volume Set, CRC, 2015 ISBN-10: 1439839778

[14] Stahl, H. Philip, "HabEx baseline telescope design and predicted performance", Proc. SPIE 11115, UV/Optical/IR Space Telescope and Instruments, August 2019.

[15] Stahl, H. Philip, Michael Effinger and Thomas Brooks, "Predictive Thermal Control study overview and accomplishments: year 2", Proc. SPIE 11116, Astronomical Optics: Design, Manufacture and Test of Space and Ground Systems, August 2019.

[16] Dohring, Hartmann, Lentes and Jedamzik, Heritage of ZERODUR® Glass Ceramic for Space Applications.

[17] Westerhoff, Thomas, and Tony Hull, "Production of 4 m diameter Zerodur® mirror substrates", HabEx White Paper Contribution, 2018.

[18] Egerman, et. al., "Status of the Advanced Mirror Technology Development (AMTD) phase 2 1.5m ULE mirror", Proc. SPIE. 9575, Optical Manufacturing and Testing XI, 95750L. (August 27, 2015) doi: 10.1117/12.2188566

[19] Cox, Charles, "Collins Aerospace Inputs and Assessment for the HabEx Primary Mirror Assembly", Document PA-2227, 12-14-2018.

[20] Harper, Brian L., Kenneth E. Hrdina, W. David Navan, Joseph Ellison, Andrew Fanning, "Measuring thermal expansion variations in ULE glass with interferometry," Proc. SPIE 5374, Emerging Lithographic Technologies VIII, (20 May 2004);

[21] R. Jedamzik, T. Westerhoff, "Homogeneity of the coefficient of linear thermal expansion of ZERODUR®: A Review of a decade of evaluations" Proc. SPIE Vol. 10401, (2017)

[22] Hall, H.D., Problems in adapting small mirror fabrication techniques to large mirrors, Optical Telescope Technology Workshop, April 1969, NASA Report SP-233, 1970.

[23] Montagnino, R. Arnold, D. Chadwick, L. Grey, G. Rogers, "Test And Evaluation Of A 60-Inch Test Mirror," Proc. SPIE 0183, Space Optics II, (27 September 1979);

[24] Krim, Michael H., "Metrology Mount Development And Verification For A Large Spaceborne Mirror," Proc. SPIE 0332, Advanced Technology Optical Telescopes I, (4 November 1982);

[25] Montagnino, Lucian A., "Test And Evaluation Of The Hubble Space Telescope 2.4-meter Primary Mirror," Proc. SPIE 0571, Large Optics Technology, (21 February 1986)

[26] https://www.hexagonkh9.com/blog/2019/1/19/hexagon-looked-at-the-earth-the-hubble-looked-at-the-stars

[27] Zinn, John W., George W. Jones, "Kepler primary mirror assembly: FEA surface figure analyses and comparison to metrology," Proc. SPIE 6671, Optical Manufacturing and Testing VII, 667105 (14 September 2007)

[28] Evans, Chris J., and Robert N. Kestner, "Test optics error removal", Applied Optics, Vol.35, No.7, 1 March 1996.

[29] Zolcinski-Couet, Marie-Christine, Joseph A. Magner, David A. Zweig, "Absolute calibration of flats for densely sampled data", Proc. SPIE 2536, Optical Manufacturing and Testing, (8 September 1995); doi: 10.1117/12.218463

[30] Kissil, Andy "SFE Correction for HabEx Primary Mirror", 12 July 2018